

# INDIVIDUAL AUTHENTICATION THROUGH HAND POSTURE RECOGNITION USING MULTI-HILBERT SCANNING DISTANCE

*Jegoon RYU and Sei-ichiro KAMATA*

Waseda University  
Graduate school of Information, Production, and Systems  
2-7, Hibikino, Wakamatu-ku, Kitakyushu-shi, Fukuoka, 808-0135 Japan  
jkryu@ruri.waseda.jp and kam@waseda.jp

## ABSTRACT

In this paper, we propose a novel Hand Posture Recognition (HPR) for biometrics. This study uses the three dimensional point clouds for robust hand posture recognition at the rotation and scale. Multi-Hilbert Scanning Distance (MHSD) are also introduced for mathematical approaches of shape matching. HPR framework is divided into five parts: detecting hand region, removing the wrist, aligning the hand pose, extracting feature descriptor, and matching. Based on the experimental results, this framework showed superior results for hand posture recognition rate.

**Index Terms**— Biometrics, Hand Posture Recognition (HPR), Hilbert Scanning, Multi-Hilbert Scanning Distance (MHSD)

## 1. INTRODUCTION

Biometric technologies for automated personal authentication have been received extensive attention in today's global information society, due to increasing security concerns and the increasing number of applications requiring reliable authentication of individual. Many physiological and behavioral traits that are inherent and unique to each individual are considered for these technologies. Features such as face, fingerprint, iris, hand geometry, palmprint, gait, voice signature, hand writing, and gesture, etc., have been suggested for reliable authentication of individual. Each biometrics has its strengths and limitations according to user acceptance, cost, performance, complexity, the security level, and etc [1]. For example, fingerprint and iris verification systems work well for high security applications, but they are not suitable for medium and low security applications due to privacy concerns and do not enjoy users acceptance. On the other hand, face or voice recognition based authentication systems prove to be cost effective for simple access control implementations, but it cannot be used in high security zones. Trade-off between these two is the hand authentication system that is cost effective and

can be considered the most suitable modality for medium and low-level security application. They do not cause anxiety for the user like fingerprint and iris systems and users are easy to accept due to their convenience. Moreover, they can be also specified with low resolution images and dirty or greasy hands don't hamper the quality of templates [2]. There are two categories for hand recognition system (HRS) according to the capture device; contact based and contact free hand biometric systems. Most of the existing hand involved techniques require pegs or contact-based image acquisition devices. This causes some increasing user acceptance issues and system reliability issues. In the study, we propose a novel framework for contact free hand biometrics using Hand Posture Recognition (HPR). This approach introduces hand posture recognition using Three Dimensional (3-D) Hand Posture Point Clouds (HPPC) and Multi Hilbert Scanning Distance (MHSD) for mathematical approaches of shape matching.

## 2. EXTRACTING THE HAND POSTURE

### 2.1. Point Clouds for Hand Posture and Hand Detection

The point clouds are usually used to represent the surface of object as sets of vertices in a 3D coordinate system. 3D information of an object can provide the scale-independent characteristic from motion pictures. A hand posture is a static hand pose and hand location without any movement involved. To obtain the hand posture point clouds, the back of one's hand is measured by stereo camera. There are two instructions for hand posture templates using capture device; (1) User takes a comfortable and specific hand posture, and one finger has to be stretched at least. (2) One puts the posed hand in the free space in front of the capture device (stereo camera), and the back of the posed hand is faced the capture device. In this study, a template of HPPC is obtained by a combination of two dimensional (2-D) and three dimensional (3-d) information. The point clouds on the captured scene are represented by the combination of 3D Cartesian coordinate system of a point, row and column information, and *rgb* color information. A hand posture region in the captured data is extracted

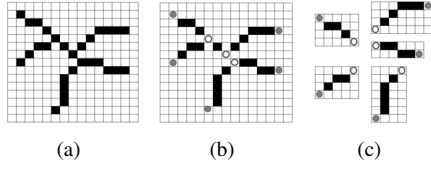


**Fig. 1.** Sub skeleton lines using end and bifurcate points.

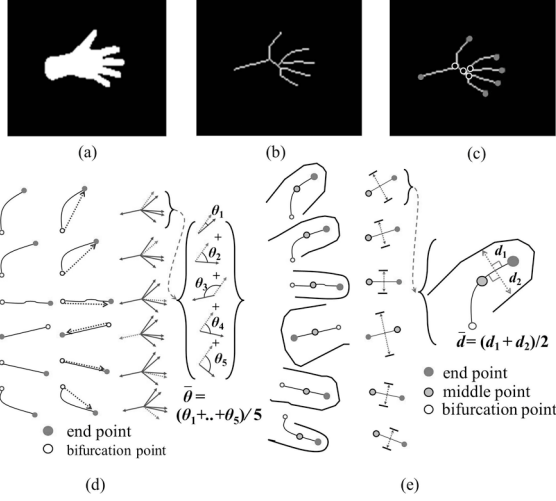


**Fig. 2.** Hand skeleton line and computation of an average angle and distance with sub skeleton lines.

using YCbCr skin color information.

## 2.2. Eliminating the Wrist in Hand Region

The hand region from section 2.1 includes the wrist region. To obtain the normalized hand posture, the elimination of the wrist is required. This section introduces seven steps for a Wrist Line Extraction (WLE) method for eliminating the wrist in hand region.

(1) *Extracting hand skeleton in binary image*: the thinning method is used as the process of skeletonization to get an image of single pixel width with no discontinuities.

(2) *Extracting sub skeleton lines*: the sub skeleton lines are obtained by endpoints and bifurcations in skeleton image. The crossing number [3] is used for detecting bifurcations and endpoints in a binary skeletonized image. Figure 1 shows the endpoints, bifurcation, and the extraction of sub skeleton lines in skeleton image. A sub skeleton line can write as follows:

$$L_j^s = p_b, p_1, p_2, p_3, \dots, p_k, p_e, j = 1, \dots, n \quad (1)$$

where  $p_b$  is the bifurcation,  $p_e$  is the endpoint, and  $p_1, \dots, p_k$  are intermediate points which are on the sub skeleton line between bifurcation and endpoint.  $n$  is the number of sub skeleton lines.

(3) *Computing a average angle between sub skeletons*: The angle factors between sub skeleton lines are computed to

**Table 1.** The pseudo-code for the wrist direction decision

```

if ( $p == q$ ) then select( $p$  or  $q$ )
else  $\gamma_A = \frac{\bar{A}_p^s}{\bar{A}_q^s}$  and  $\gamma_D = \frac{D_p^s}{D_q^s}$ 
if  $\gamma_A > \lambda$  then select( $p$ )
else if  $\gamma_A > \gamma_D$  then select( $p$ )
else select( $q$ )
end if
end if

```

§  $p$  is the index of max average subtraction angle,  $q$  is the index of max distance,  $\bar{A}_p^s$  is the average angle for  $p$ -th skeleton line,  $\bar{A}_q^s$  is the angle for  $q$ -th skeleton line,  $D_p^s$  is the distance for  $p$ -th skeleton line,  $D_q^s$  is the distance for  $q$ -th skeleton line,  $\gamma_A$  is a angle ratio,  $\gamma_D$  is a distance ratio,  $\lambda$  is a threshold value for the sub skeleton line of the wrist.

decide the sub skeleton for the wrist. Each sub skeleton line has a direction vector  $\vec{d} = \overrightarrow{p_b p_e}$  by bifurcation and endpoint. Angle  $\theta_{ji}^s$  between the direction vector  $\vec{d}_j$  for a sub skeleton line and the direction vector  $\vec{d}_i$  for another sub skeleton lines is calculated as follows:

$$\theta_{ji}^s = \arccos\left(\frac{\vec{d}_j \cdot \vec{d}_i}{|\vec{d}_j| |\vec{d}_i|}\right) \quad (2)$$

and average angle between the  $j$ -th direction vector and the other direction vectors is as follows:

$$\bar{A}_j^s = \frac{1}{n} \sum_{i=1}^n \theta_{ji}^s \quad (3)$$

$$\bar{A}_M^s = \max(\bar{A}_j^s), j = 1, \dots, n \quad (4)$$

where  $\bar{A}_M^s$  is the max angle among  $\bar{A}_j^s, j=1, \dots, n$ , and  $n$  is the number of sub skeleton line.

(4) *Computing a distance between each sub skeleton and hand contour*: As the other factor for deciding the sub skeleton for the wrist, the distance  $D^s$  between sub skeleton line and hand contour is computed.  $D^s$  is computed as the distance from  $p_k$  to hand contour point by the normal direction of  $\overrightarrow{p_e p_m}$ .  $p_m$  is the middle point between bifurcation and endpoint on sub skeleton line, and  $m$  is the half of the number of intermediate points.  $hp$  is the half point between the endpoint  $p_e$  and middle point  $p_m$  on sub skeleton line.

$$D_j^s = \text{dist}(hp_j, p_{\text{contour}}) \quad (5)$$

$$D_M^s = \max(D_j^s), j = 1, \dots, n \quad (6)$$

where  $D_M^s$  is the max distance among  $D_j^s, j=1, \dots, n$ , and  $n$  is the number of sub skeleton line.

(5) *Deciding the sub skeleton  $L_w^s$  for the wrist direction*: Two factors from step (3) and step (4) are used for determining the direction of the wrist in hand region. In Table1, the pseudo code presents for deciding the sub skeleton.

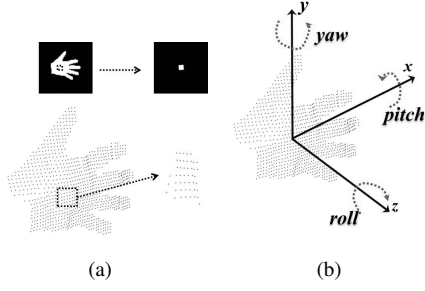


**Fig. 3.** A sub region of the back of one's hand in HPPC and rotation for alignment of hand posture.

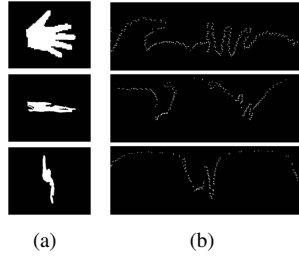


**Fig. 4.** Three view binary image projected from HPPC and polar transformation. The front, top, and left view image.

(6) *Extracting the center point on the palm:* In hand region, the center point  $p_c$  is extracted using the distance map. The mask operation  $\otimes$  for the distance map  $dm$  is just performed in the temporary region in hand region. The temporary region is as follows:

$$tr = \left( \bigcup_j^n C_{p_b^j} \right) \cap H^b \quad (7)$$

$$p_c = \text{centroid}(\max(tr \otimes dm)) \quad (8)$$

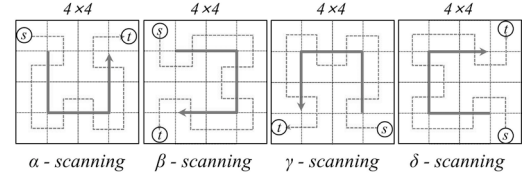
where  $tr$  is the temporary region for center point on palm,  $C_{p_b^j}$  is the circle region for the radius  $l$  from bifurcation  $p_b^j$ ,  $n$  is the number of bifurcation, and  $H^b$  is the binary hand region.

(7) *Extracting the wrist line:* the wrist line is extracted using the center point  $p_c$  and the sub skeleton line  $L_w^s$  for the wrist. A circle for radius  $r$  from center point  $p_c$  intersects with the sub skeleton line for the wrist. The intersection point is  $p_{int}$ . Thus, the wrist line can be extracted by calculation of the tangent for  $p_{int}$  on the circle.

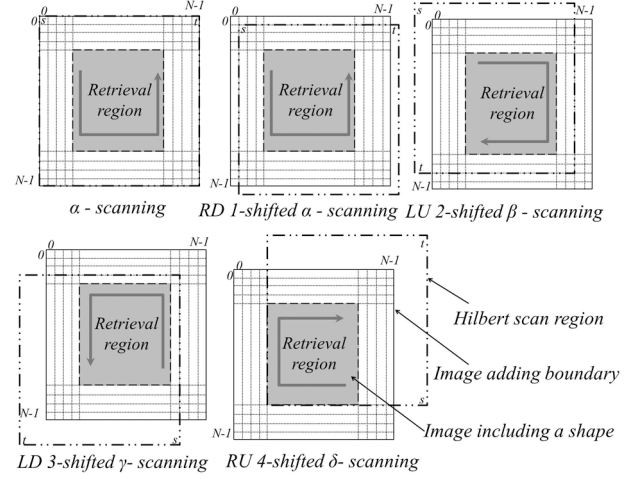
### 3. FEATURE EXTRACTING AND MATCHING

#### 3.1. Aligning and Projecting the HPPC

The normal vector for a surface of HPPC is computed for aligning the HPPC. In 3D subspace, the normal vector can be easily computed if we use the assumption that the  $z$  coordinate is functionally dependent on the  $x$  and  $y$  coordinates.



(a)



(b)

**Fig. 5.** Four directional Hilbert scans and multi-Hilbert scans.

Given the set of  $n$  points  $\mathbf{S} = [\mathbf{x}, \mathbf{y}, \mathbf{z}]^T = [x_1 \cdots x_n, y_1 \cdots y_n, z_1 \cdots z_n]^T$  from point clouds, best fitted plane is capable of being calculated by Least Square Fitting [4]. The normal vector associated with the surface  $\mathbf{S} = [\mathbf{x}, \mathbf{y}, \mathbf{z}]^T$  is represented  $\hat{\mathbf{n}} = [\hat{p}, \hat{y}, \hat{r}]^T$ . Figure 3 shows the alignment of HPPC using the normal vector. The aligned hand posture is projected into three planes ( $xy, yz, xz$ -plane). Figure 4 shows the projected hand posture images on  $xy, yz$ , and  $xz$ -plane, respectively. Lastly, The projected images are transformed into polar coordinates.

#### 3.2. Matching using Multi-Hilbert Scanning Distance

The Hilbert scanning distance [5] was utilized for a accurate and fast measurement of the similarity between two point sets on a 2-D image. However, the HSD has some drawbacks in accurate shape recognition. Thus, multi-Hilbert scanning distance is introduced to overcome HSD and perform accurate shape recognition. There are four types of Hilbert scans of an image. In this study,  $\alpha$ -scanning,  $\beta$ -scanning,  $\gamma$ -scanning, and  $\delta$ -scanning are named according to the scanning direction. Figure 5(a) shows the four directional Hilbert scans. Figure 5(b) illustrates the retrieval region and the Multi-Hilbert Scanning (MHS) of an image. MHS consists of five scan types: a single directional Hilbert scanning and the diagonally shifted scans of the

four directional Hilbert scans (Right-Down (RD) 1-shifted  $\alpha$  - scanning, Left-Up (LU) 2-shifted  $\beta$  - scanning, Left-Down (LD) 3-shifted  $\gamma$  - scanning, and Right-Up (RU) 4-shifted  $\delta$  - scanning). Given two finite point sets  $P = \{p_0, \dots, p_{M-1}\}$  and  $R = \{r_0, \dots, r_{L-1}\}$  where  $p$  ( $p \in P$ ) and  $r$  ( $r \in R$ ) have integer coordinates in an image, the point sets are converted by the MHS into two new point sets  $A = \{A^\alpha, A^{RD-\alpha}, A^{LU-\beta}, A^{LD-\gamma}, A^{RU-\delta}\}$  and  $B = \{B^\alpha, B^{RD-\alpha}, B^{LU-\beta}, B^{LD-\gamma}, B^{RU-\delta}\}$  in a 1-D sequence.  $A^\alpha = \{a_0^\alpha, \dots, a_{M-1}^\alpha\}$  and  $B^\alpha = \{b_0^\alpha, \dots, b_{L-1}^\alpha\}$  are the point sets given by  $\alpha$  - scanning of  $P$  and  $R$ , respectively. The distances  $d_\alpha(A^\alpha, B^\alpha), d_{RD-\alpha}(A^{RD-\alpha}, B^{RD-\alpha}), d_{LU-\beta}(A^{LU-\beta}, B^{LU-\beta}), d_{LD-\gamma}(A^{LD-\gamma}, B^{LD-\gamma}),$  and  $d_{RU-\delta}(A^{RU-\delta}, B^{RU-\delta})$ , which are the sets of distances for each point in  $A^\alpha, A^{RD-\alpha}, A^{LU-\beta}, A^{LD-\gamma},$  and  $A^{RU-\delta}$ , are computed by

$$d_f(A^f, B^f) = \{\min_j \|a_i^f - b_j^f\|\}, \quad (9)$$

$$i = 0, \dots, M-1 \text{ and } j = 0, \dots, L-1$$

where  $f$  denotes the five scans types.  $\|\cdot\|$  is the Euclidean norm distance in 1-D space. The directed  $h_{mhsd}(A, B)$  from A to B is computed by

$$h_{mhsd}(A, B) = \frac{1}{M} \sum_{i=0}^M \min(d_f(A^f, B^f)). \quad (10)$$

where  $M$  is the number of points in the point set  $A$ . The directed  $h_{mhsd}(B, A)$  from B to A can be computed similarly. MHS is defined as the following:

$$H_{mhsd}(A, B) = \max(h_{mhsd}(A, B), h_{mhsd}(B, A)). \quad (11)$$

#### 4. EXPERIMENTAL RESULTS AND DISCUSSION

In this study, 45 subjects were involved from the experiments. The hand posture is measured six times for each subject as changing the directional angle and the location. Figure 6 shows five samples of the data-set. The proposed method with MHS is compared with HD and MHD for recognition rate. In order to evaluate the proposed methods, the Cumulative Match Scores (CMS) rank order statistic is measured. Table 2 shows the comparison with HD and MHD [6][7]. As a result, the MHD showed the good recognition rate. Nevertheless, the proposed method demonstrates a superior result than other methods.

**Table 2.** Comparison of hand posture recognition rates

Methods	Ranking 1(%)	Ranking 5(%)
HD	85.1	90.7
MHD	92.5	96.2
Proposed method	95.9	98.5



**Fig. 6.** Five samples for hand posture data-set.

#### 5. CONCLUSION

In summary, this study proposed a novel framework for contact-free based hand biometrics using hand posture recognition. 3-D HPPC was used for HPR, and WLE was introduced for obtaining a template of the hand posture. MHS was also introduced for mathematical approaches of shape matching. Based on the experimental results, this framework showed superior results for HPR rate.

#### 6. REFERENCES

- [1] A.K. Jain, A. Ross, S. Prabhakar, "An introduction to biometric recognition," IEEE Trans. Circ. Sys. Video Technol., vol. 14, no. 1, pp. 4-20, 2004.
- [2] N. Duta, "A survey of biometric technology based on hand shape," Pattern Recognition, vol. 42, pp. 2797-2806. 2009.
- [3] D. Maltoni, D. Maio, A.K. Jain, and S. Prabhakar, Handbook of Fingerprint Recognition, 2nd ed. Springer Publishing Company, Incorporated, 2009.
- [4] A. Bjorck, Numerical methods for least squares problems, SIAM, 1996.
- [5] L. Tian, S. Kamata, K. Tsuneyoshi, and H.J. Tang, "A fast and accurate algorithm for matching images using Hilbert scanning distance with threshold elimination function," IEICE Trans., vol. E89-D, no. 1, pp. 290-297, 2006.
- [6] D.P. Huttenlocher, G.A. Klanderman, W.J. Rucklidge, "Comparing images using the Hausdorff distance," IEEE Trans. Pattern Anal. Mach. Intell., vol. 15, pp. 850-863, 1993.
- [7] M.P. Dubuisson, A.K. Jain, "A modified Hausdorff distance for object matching," in 12th International Conference on Pattern Recognition, 1994, pp. 566-568.